

UNCLASSIFIED

AD NUMBER	
AD517038	
CLASSIFICATION CHANGES	
TO:	unclassified
FROM:	secret
LIMITATION CHANGES	
TO:	Approved for public release, distribution unlimited
FROM:	Controlling DoD Organization: Air Force Cambridge Research Labs., Hanscom AFB, MA.
AUTHORITY	
OL-AA PL/GPS 1tr dtd 8 Nov 1995; OL-AA PL/GPS 1tr dtd 8 Nov 1995	

THIS PAGE IS UNCLASSIFIED

AD-517038

AFCRL-71-0221
30 MARCH 1971
AIR FORCE SURVEYS IN GEOPHYSICS, NO. 233

EXCLUDED FROM AUTOMATIC REGRADING:
DOD DIR 5200.10 DOES NOT APPLY



SPACE PHYSICS LABORATORY PROJECT ILIR

AIR FORCE CAMBRIDGE RESEARCH LABORATORIES

L. G. HANSCOM FIELD, BEDFORD, MASSACHUSETTS

(U) Project EGAD, Exploratory Geophysical Anomaly Detection

R.O. HUTCHINSON

This research was supported by the AFCRL Laboratory Director's Fund

This material contains information affecting the national defense of the United States within the meaning of the Espionage Laws (Title 18, U.S.C., Sections 793, 794) the transmission or revelation of which in any manner to an unauthorized person is prohibited by law.

In addition to security requirements which apply to this document and must be met, each transmittal outside the Department of Defense must have prior approval of AFCRL, XO, L.G. Hanscom Field, Bedford, Massachusetts 01730.

AIR FORCE SYSTEMS COMMAND
United States Air Force



Copy No. 22

Reproduced From
Best Available Copy

19990303149

(This page is unclassified)

Abstract

(U) An airborne reconnaissance magnetometer system (ARMS) was installed in a Grumman Tracker (S2E) aircraft in a joint program with the Naval Air Development Center, Johnsville-Warminster, Pa. Signatures were obtained from targets of special interest and magnetic moments were computed from the flight data and compared with values derived from theoretical considerations. Signal amplitude, noise amplitude, signal period, and relative signal-to-noise ratio were obtained for each signature by passing the recorded signals through a series of half-octave filter steps. Suggestions for optimum filtering are presented. Anti-Submarine Warfare (ASW) signal processing techniques were investigated to determine their usefulness for land target identification. Applications of the ARMS and EGAD systems and recommendations for future investigations are given.

In addition to security requirements which apply to this document and must be met, each transmittal outside the Department of Defense must have prior approval of AFCEC, HQ, L.S. Hanscom Field, Bedford, Massachusetts 01732.

Qualified requesters may obtain additional copies from the Defense Documentation Center.

[REDACTED]

[illegible]

1. *Chlorophyll a* and *Chlorophyll b* were determined by the method of Arar and Collins (1971) using a Shimadzu 1601 UV-Visible Spectrophotometer. The concentration of chlorophyll was expressed in $\mu\text{g mL}^{-1}$.

the 1990s, the number of people in the world who are under 15 years of age is expected to increase from 1.1 billion to 1.5 billion. The number of people aged 65 and over is expected to increase from 200 million to 400 million. The number of people aged 15 and over is expected to increase from 3.5 billion to 4.5 billion. The number of people aged 15 and over is expected to increase from 3.5 billion to 4.5 billion. The number of people aged 15 and over is expected to increase from 3.5 billion to 4.5 billion.

Journal of Management Studies, 36(7), 809–826.

Illustrations

Frontispiece. Applications of Aeromagnetic Detection	viii
1. Vandenberg AFB, Titan Sites 395-C and 395-D	5
2. Vandenberg AFB, Minuteman Sites 05, 07, 22	6
3. Direct Signal, Titan II Site 3-5, McConnell AFB	9
4. Processed Signal, Site 3-5, for Filters 1-8	10
5. Signature Frequency and Period vs Altitude and Ground Speed	11
6. Signal Strength vs Target Distance	14
7. Signal Characteristics vs Time in Seconds	15
8. ARMS Signal vs Time	16
9. Relative Signal + Noise and Noise Levels vs Filter Numbers	18
10. Filter Number vs Altitude for Maximum Signal and Signal/Noise	19
11. NADC Data Analysis Flow Chart	21

Tables

1. Filter Frequencies and Periods	8
2. Information Tabulated for Each Pass	11
3. Magnetic Moments of Various Targets	12
4. NADC Data Collection Summary	20
5. NADC Target Dipole Moments	21
6. Auto-Detection of EGAD Targets	22

PRECEDING PAGE BEANK NOT FILMED.

(This page is unclassified)

Contents

1. INTRODUCTION, OBJECTIVES, AND RELEVANCE	1
2. TECHNICAL APPROACH	2
2.1 Flight Test Plan	3
2.2 Areas of Operation	3
3. DATA PREPARATION AND ANALYSIS	8
3.1 AFCRL Procedures	8
3.2 NADC Procedures	20
4. CONCLUSIONS	22
5. APPLICATIONS	23
6. RECOMMENDATIONS	24
ACKNOWLEDGMENTS	25
REFERENCES	27
APPENDIX A. ZIL Signatures	29

[REDACTED]

[REDACTED]

[REDACTED]

(U) Project EGAD
Exploratory Geophysical Anomaly Detection

1. INTRODUCTION, OBJECTIVES, AND RELEVANCE

(S) The application of aeromagnetic detection techniques to counter-insurgency warfare was discussed by Maple (1966) in a preliminary technical paper. It was shown that the field of a likely target could be approximated by that of a magnetic dipole for the sensor to target distances normally employed in aeromagnetic detection. Available and potentially available sensors and their sensitivities were reviewed and methods of estimating target dipole moments based on size and shape factors were presented. Zawalick and Hutchinson (1970) reported on a series of flight tests in the United States over areas analogous to specific areas within Southeastern Asia. Permanent and induced fields, resultant magnetic moments, and ranges of variation for target vehicles were studied. Signatures were obtained for various combinations of target size, spacing, heading, and distances. Then analytic expressions were derived for target signatures and compared with the experimental values. This paper is concerned chiefly with the extension of these techniques to the problem of detecting ballistic missile launch sites.

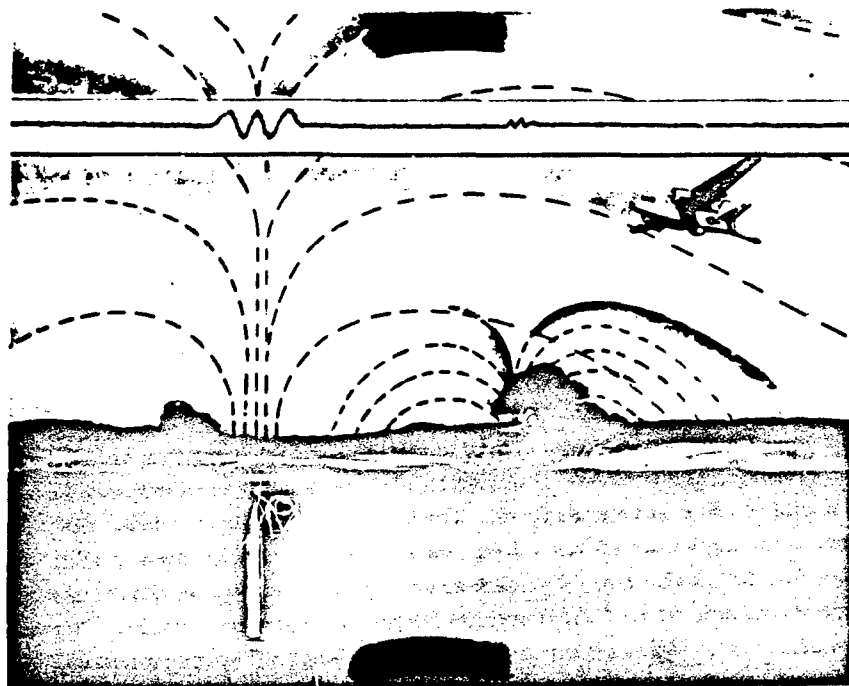
(S) The primary objective of EGAD was to detect the presence of ballistic missile launch silos by means of their magnetic signatures. Secondary objectives were to attempt to differentiate between empty or loaded silos and fired or unfired

(Received for publication 30 March 1971)

[REDACTED]

[REDACTED]

PRECEDING PAGE BLANK. NOT FILMED.



Frontispiece. Application of Aeromagnetic Detection (U)

SECRET

3

(U) The output from each filter system was recorded on a separate track of the flight tape recorder. A third track was utilized for voice recording of target, heading, altitude, ground speed, and other pertinent data. In addition, the ARMS and NADC filter outputs were recorded on a dual-trace strip chart providing visual information for equipment operators.

2.1 Flight Test Plan

(S) Multiple level flights with cardinal and intercardinal heading patterns, direct and offset, were planned for each distinct target type. The normal ASW cloverleaf search pattern with its 270° right hand turns was to be used as much as possible with a straight and level flight attitude being maintained for at least a mile preceding and following the on-top or nearest approach point. Specific target types desired follow:

- a. Minuteman
 - (1) An empty silo that has never been used for a firing.
 - (2) The same or a very similar silo containing a missile.
 - (3) An empty silo that has been used for several test firings.
 - (4) The same or a very similar silo containing a missile.
- b. Titan II
 - (1) An empty silo that has never been used for a firing.
 - (2) The same or a very similar silo containing a missile.
 - (3) An empty silo that has been used for several test firings.
 - (4) The same or a very similar silo containing a missile.
- c. A Russian built ZIL-157 truck
 - (1) Heading N
 - (2) Heading S
 - (3) Heading E
 - (4) Heading W
- d. Overflights above a normally dispersed operational wing of
 - (1) Minuteman missiles
 - (2) Titan II missiles

2.2 Areas of Operation

(U) Flight operations were conducted in four areas: Vandenberg AFB, Calif.; White Sands, N. M.; McConnell AFB, Kansas, and Whiteman AFB, Mo. The aircraft was based at NAS, Point Mugu, Calif., and then at Kirtland AFB, N. M., for support and maintenance during the tests at the first two areas, respectively, and at the named bases for the last two areas cited.

SECRET

silos by means of small differences in magnetic signatures. An additional objective was to continue Project ARMS, a truck interdiction program with special emphasis on the magnetic properties of a Russian built ZIL 157 vehicle.

(S) This project is relevant to both immediate and future Air Force systems and programs because it would make possible:

- (a) the detection of ballistic missile launch sites in "friendly" or neutral areas from manned or drone aircraft;
- (b) a kind of airborne inspection of supposed missile sites as a means of checking on a weapons ban treaty without violating a nation's ground sovereignty;
- (c) an evaluation of the possibility of using the magnetic signature of a silo to provide terminal guidance for incoming destructive weapons;
- (d) post-strike reconnaissance of an aggressor's territory after a nuclear exchange to determine his additional strike capability and to obtain targeting information;
- (e) an all-weather, passive, non-jammable truck interdiction system.

2. TECHNICAL APPROACH

(U) A Varian ARMS magnetometer system (McBride 1967, 1968) was installed in a Grumman tracker (S2E) aircraft in a joint program with the Naval Air Development Center, Johnsville-Warminster, Pa. This aircraft is the current fleet anti-submarine warfare unit and has been subjected to special methods of magnetic compensation including the installation of a nine term compensator. The sensing head was mounted in the extendable boom and the control system, memory tube system, strip chart recorder, and magnetic tape recorder were installed in the aircraft.

(U) Each pass of the aircraft along a straight flight line passing near a target produced a plot or profile of magnetic field strength vs distance. The length of the target profile was determined by the target distance that was normally only slightly greater than the altitude of the aircraft. The length and shape of the target profile and the aircraft ground speed then determine the frequency content of the signal. Bandpass filtering is incorporated in the detector to eliminate most of the normal background noise while retaining as much of the desired signal as possible. The ARMS filter system was modified to provide optimum bandpass settings for the expected target conditions. The -3dB points for the high-pass filter section were changed to 0.015, 0.025, 0.035, 0.25, and 0.50 Hz while the low-pass filter settings remained at 0.5, 1.0, 1.5, and 2.0 Hz. Similar modifications were made to the NADC Butterworth land target filter package which also incorporated provisions for adjusting the roll-off rate outside of the bandpass.

FOR OFFICIAL USE ONLY

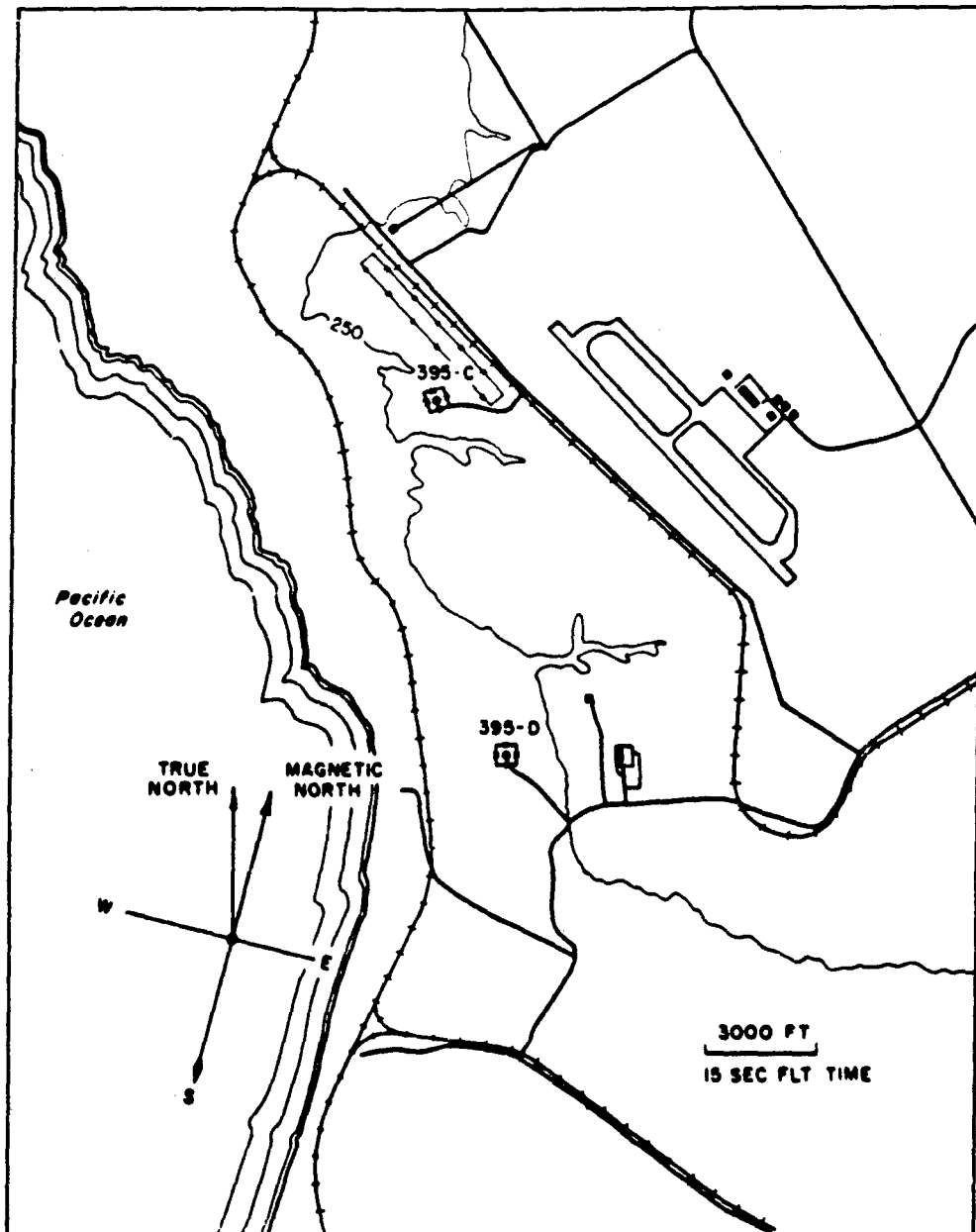


Figure 1. Vandenberg AFB, Titan Sites 395-C and 395-D (U)

SECRET

4

2.2.1 VANDENBERG AFB, CALIFORNIA

(S) Titan II Pads No. 395-C and No. 395-D were selected for the initial tests; their location permitting moderately clean approaches and runouts on the cardinal magnetic headings. Surface elevations were 280 and 170 ft respectively and declination, $D = 15.7^{\circ} E$, total magnetic intensity, $F = 50,500\gamma$, and inclination $I = 60^{\circ}$. Both sites contained operational missiles during the test period and both sites had been used for test shots many times previously. Figure 1 shows the location of the Titan pads relative to the shore line, the Southern Pacific rail lines, base roads, and the airstrip. The 250 ft topographic contour is also shown along with a compass rose oriented to the cardinal magnetic headings to illustrate planned flight lines. Soil borings in the vicinity of the silos showed silty sands or a sand-silt mixture over a locally indurated windblown sand.

(S) Minuteman pads are shown in Figure 2. They are located between the shore line and a series of abruptly rising hills to the east and northeast. These factors, along with the close spacing of the pads and the area geology, made clean signal acquisition difficult. Passes were flown over sites 05, 07, and 22, their surfaces being at elevations of 100 ft, 135 ft, and 175 ft, respectively. Each of these pads had been used for several firings; site 22 had launched its bird one day prior to the EGAD tests, site 07 was loaded throughout the test period, and site 05 was empty. Borings near 07 showed fine sands, silty sands, and sandy clays while those near 05 and 22 showed gravel, sand, and clay mixtures.

(S) The geology of the area containing the Minuteman tubes is complex. Although terrace sands, sandstone, siltstone, and conglomerates predominate there is an igneous rock intrusion, trending E - W about 1000 ft north of 07. Terrace sands predominate beneath 05 and 22 with a fault striking E - W about 1000 ft east of 07 and 3000 ft north of 22. The north or upthrown side of the fault, the Franciscan formation, consists of a dark green sandstone, black shale, chert, and basalt and is most likely moderately magnetic. The south or downthrown side consists of hard and soft shales and marine limestone beds increasing the apparent magnetic susceptibility contrast.

2.2.2 WHITE SANDS, N.M.

(S) The Air Force Weapons Laboratory, Kirtland AFB, N.M., was directed to perform an overall signature study on a Russian built ZIL-157, 6 by 6 truck of the type commonly in use in Southeast Asia for service on unimproved roads. AFCRL agreed, as a continuation of ARMS and at the time of deployment of the EGAD aircraft, to obtain aeromagnetic signatures and to determine the truck's magnetic moment. In order to provide proper security for the tests, the truck itself being classified, operations were conducted at Stallion Site, a remote installation within the White Sands test area.

SECRET

(S) Located about 95 miles south of Albuquerque at an elevation of 4800 ft the declination was 12.5°E , total magnetic intensity $52,000\gamma$, and inclination 61° . A low-level test flight from Kirtland to Stallion revealed very high levels of magnetic noise within the land target filter bandpass. The test area was very nearly flat but the underlying material, composed of lava flows and weathered deposits washed down from adjacent peaks, contributed to the high noise levels. A series of passes over various areas near the Stallion site airstrip disclosed a small section where the average noise level in the full Varian ARMS band pass of 0.015 to 2.0 Hz was just under 1γ . The target truck was placed in the center of this area and the tests were completed in accordance with the flight plan.

2.2.3 MCCONNELL AFB, KANSAS

(S) McConnell AFB is headquarters for the Titan II Wing dispersed throughout the gently rolling farm lands south and east of Wichita, Kansas. Site 3-6, elevation 1309 ft, was picked as the prime target because of its undisturbed location. A circle with a radius of five miles, centered on the silo, contains portions of only two hard surfaced roads, a few scattered dwellings, no railroads, and a handful of small masonry and earth dams. There are oil wells near the outer perimeter of the circle but no storage tanks or processing facilities of any size.

(U) Surface soils are rich and productive with abundant surface water, and the geology consists of mostly conforming sediments with low magnetic susceptibility contrasts. Declination was 9.5°E , total magnetic intensity was $55,500\gamma$, and inclination was 67° .

2.2.4 WHITEMAN AFB, MO.

(S) Whiteman AFB is located in Johnson County, west central Missouri, just south of the town of Knobnoster. It is surrounded by large numbers of Minuteman silos dispersed throughout the area and separated from each other by five to ten miles. Sites F7, F8, and F9 are located south of the base and are on the outer edge of the silo area facilitating undisturbed target approaches. Surface elevations are 878 ft, 817 ft, and 818 ft respectively. Magnetic declination is 7.5°E , total magnetic intensity is $56,500\gamma$, and inclination is 69° .

(U) The surface relief is gentle, the topsoil is rich, and the vegetation is almost lush with numerous creeks and ponds. Area roads are mostly light duty or unimproved dirt and dwellings are widely separated. There are no heavy duty roads or railroads in the immediate vicinity of the target sites.

(U) Pennsylvanian rock predominates through Johnson County. It consists of shales, clays, sandstones, and coal. The sandstone is quarried for building use and both active and abandoned pit and strip mining operations abound near Knobnoster. Small quantities of oil and low pressure gas deposits have been found at shallow depths throughout the area.

FOR OFFICIAL USE ONLY

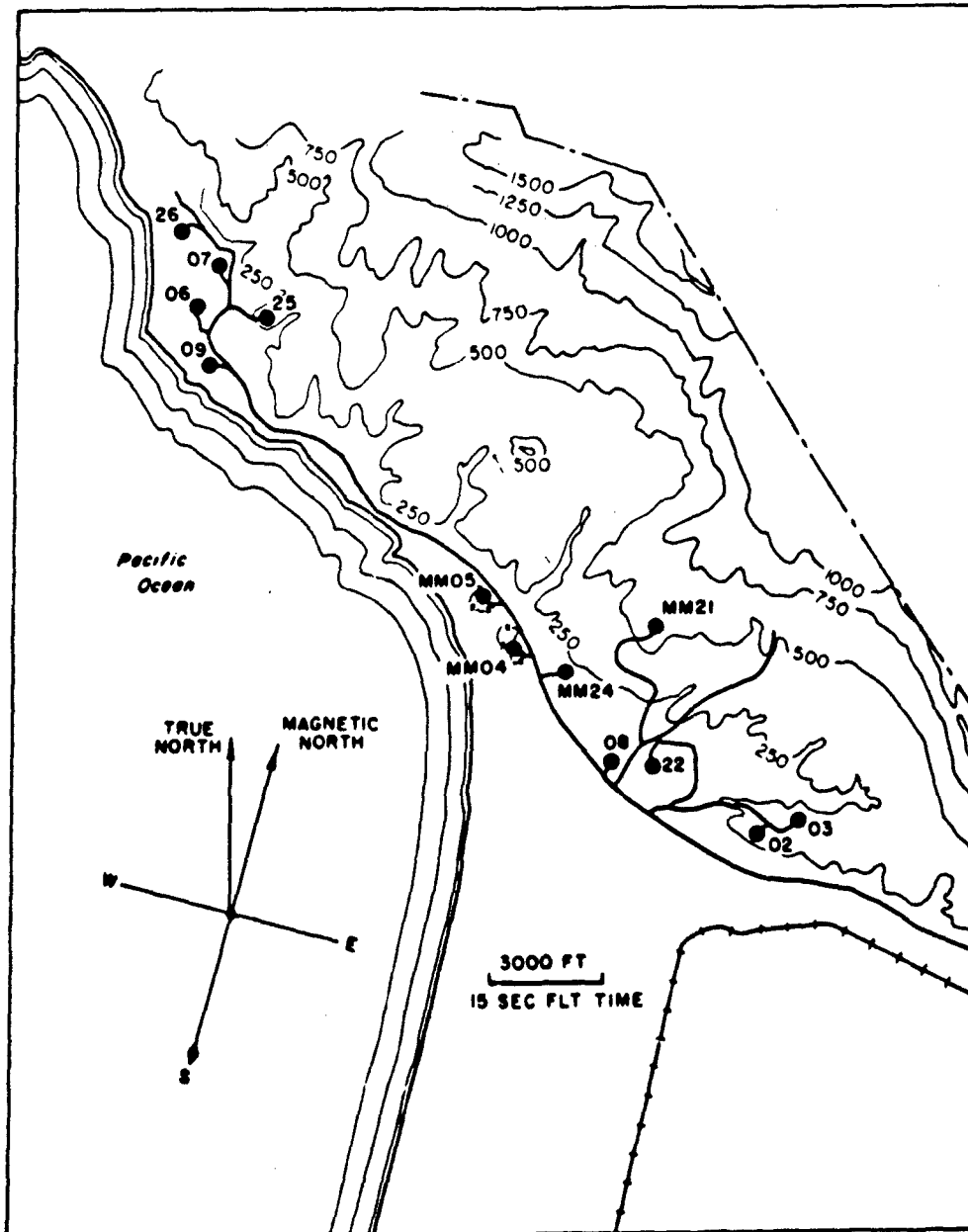


Figure 2. Vandenberg AFB, Minuteman Sites 03, 07, 22 (U)

SECRET

9

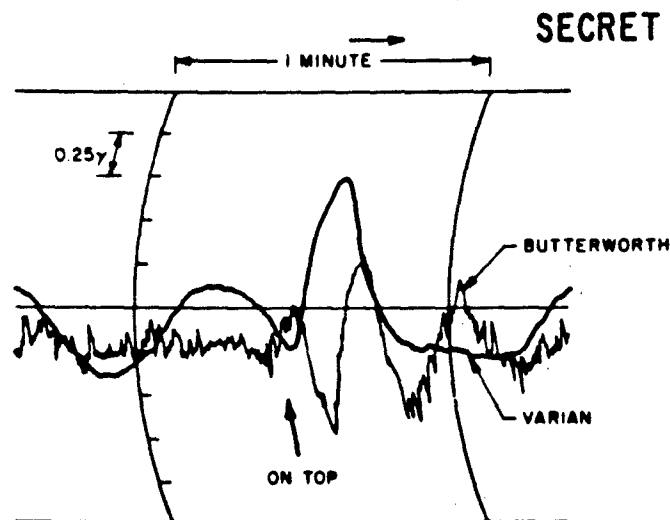


Figure 3. Direct Signal, Titan II Site 3-5, McConnell AFB (U)

(S) The Varian trace illustrates how too low a frequency filter passband increases relative geologic and maneuver noise levels and the Butterworth trace illustrates how too high a frequency allows much aircraft noise to pass. A comparison of the characteristics of the signal and noise levels passed by both filters suggests that a passband of about 0.05 to 1.0 Hz would be optimum.

(S) Figure 4 illustrates how additional selective filtering can improve visual detection for a given signal. The output of the Varian filter, as recorded on one channel of the flight tape recorder was played back through filters numbered 1 to 8 as listed in Table 1. Relative amplification for each filter channel is given above the appropriate trace in Figure 4; chart speed was 1 mm/sec. Maximum signal amplitude occurs in the passband of filter No. 2, maximum noise in No. 1 and best signal + noise to noise ratio in No. 4.

(C) Data from the original strip charts were then combined with the data from the magnetic tapes as played back through the filter bank and a master data tabulation was prepared. Table 2 lists the information scaled or noted for each pass. The data contained in this listing then became the basis for the determination of the magnetic moments of the various targets and of the optimum filter configurations for target detection in the presence of the various nontarget noise sources. Figure 5 is a theoretical plot of signature frequency and period vs altitude and ground speed. The tabulated data is in general agreement with this

SECRET

3. DATA PREPARATION AND ANALYSIS

(U) In-flight data collected, consisting of over 250 individual passes as received through both the Varian and Butterworth band pass filters were recorded on strip charts and magnetic tape. AFCRL and NADC working independently processed the data in various ways as described below.

3.1 AFCRL Procedures

(U) Each pass was first identified by means of a date and pass number cross-checking strip-chart annotations against the notebooks of the operators and the voice track of the tape recorder. The magnetic tapes were then played back through eight individual half-octave band-pass filters (White Instrument Labs. Type 1583) and recorded on an eight-channel chart recorder. Table 1 lists the frequencies and corresponding periods of the ten filters used. In normal practice, signals from the higher altitude passes were processed through filters 1 to 8 and those from the lower altitude passes through filters 3 to 10.

Table 1. Filter Frequencies and Periods (U)

Filter No.	f, in Hz	t, in secs
1	.0220 to .0312	45.5 to 32.1
2	.0312 to .044	32.1 to 22.7
3	.044 to .0625	22.7 to 16.0
4	.0625 to .0885	16.0 to 11.3
5	.0885 to .125	11.3 to 8.0
6	.125 to .177	8.0 to 5.6
7	.177 to .250	5.6 to 4.0
8	.250 to .350	4.0 to 2.9
9	.350 to .50	2.9 to 2.0
10	.50 to .71	2.0 to 1.4

(S) Figure 3 shows the data signal as received on the strip chart recorder in the aircraft for a pass over site 3-5 at McConnell AFB. Magnetic heading is 215° , altitude above sea level is 3500 ft and ground speed is 144 knots. The Varian filter bandpass was 0.025 to 1.0 Hz and the Butterworth filter was set for 0.05 to 2.3 Hz with roll-off set at 35 dB, per octave. Full scale output for both traces was 2.5 gamma. Recorder speed was three inches per minute. The Butterworth filter output was inverted, the Varian filter output was not hence the apparent phase difference between the two curves.

SECRET

(This page is unclassified)

11

Table 2. Information Tabulated for Each Pass (U)

Date	Butterworth Filter Bandpass
Pass Number	Butterworth Sensitivity
Target	Butterworth Filter Roll-off
Target Condition	Butterworth Signal Amplitude
Magnetic Heading	Butterworth Signal Period
AC Altitude	Butterworth Noise Amplitude
AC Ground Speed	Magnetic Tape Number
Varian Filter Bandpass	Original Strip Chart Number
Varian Sensitivity	Eight-Channel Strip Charter Number
Varian Signal Amplitude	1/2 Octave Filter No. for maximum signal amplitude
Varian Signal Period	1/2 Octave Filter No. for maximum background noise
Varian Noise Amplitude	1/2 Octave Filter No. for maximum S/N
Other Comments	

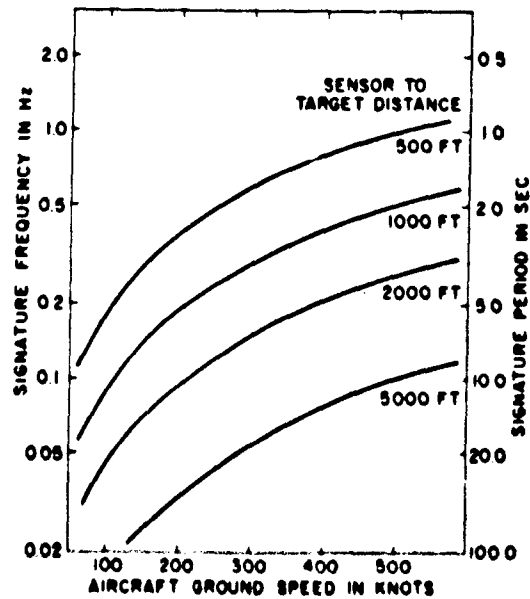


Figure 5. Signature Frequency and Period vs Altitude and Ground Speed

SECRET

SECRET

10

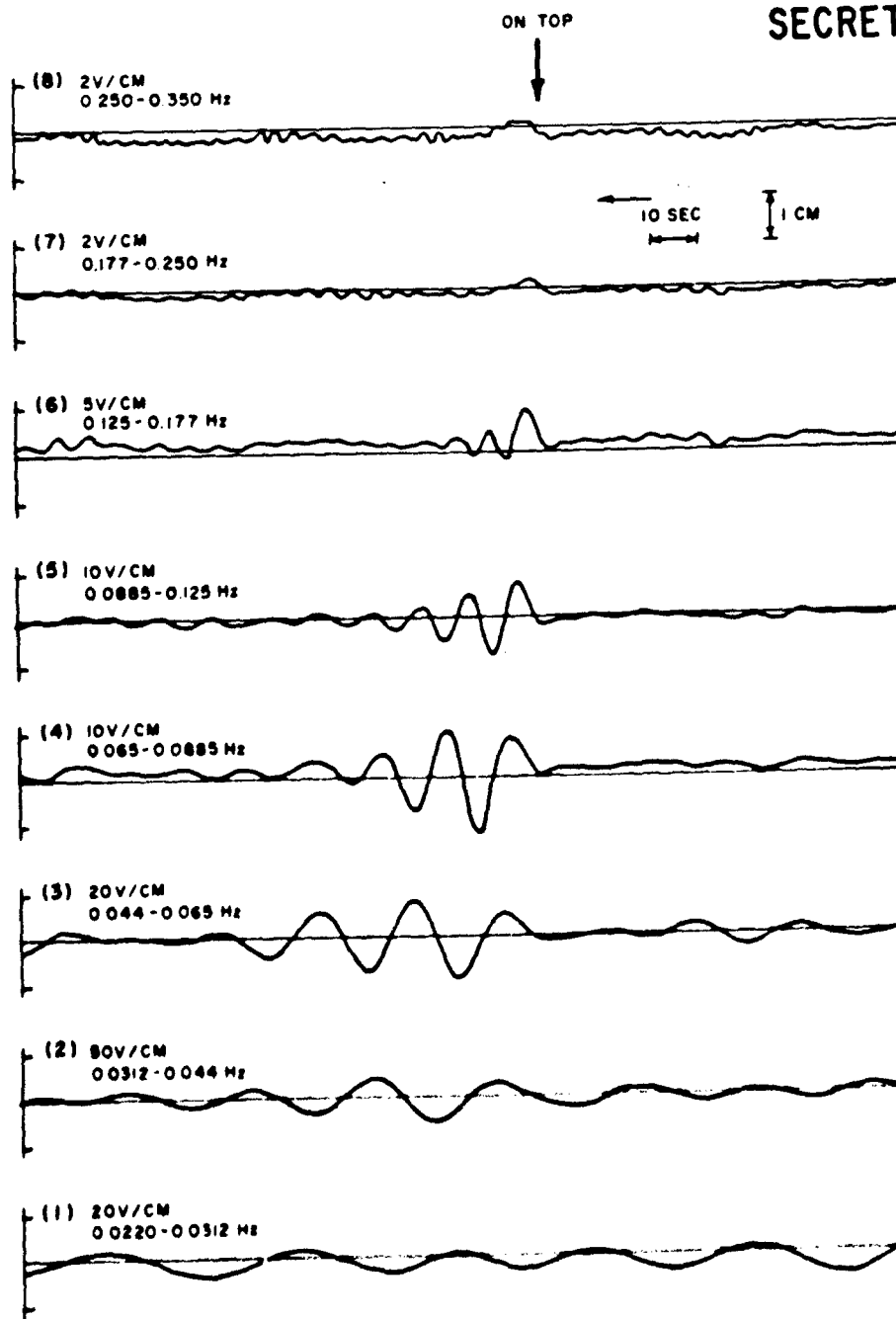


Figure 4. Processed Signal, Site 3-3, for Filters 1-8 (U)

SECRET

(S) Several entries require additional clarification or comment. The theoretical approximation for Vandenberg AFB target 395-C was based on information obtained from the construction estimates and bills of material on file at the Ralph M. Parsons Company, Los Angeles, Calif. This site contains nearly 1800 tons of ferrous materials distributed among the silo, its installed equipment, the blast locks, control center, cableway, security fencing, and a number of ring beams used during site excavation and left in place upon completion of the launch facility. The construction drawings show that about 800 tons of this material is contained in the silo mostly between the inner and outer walls with the remaining 1000 tons distributed throughout the launch complex. Assuming a cylindrical shape and a length to diameter ratio of unity for the larger mass of material outside the silo, one unit of 200 tons in the inner silo tube with an L/D of 5, one unit of 600 tons with an L/D of 2, and the numerical values given in Tables 2 and 3 of Maple (1966) we obtain respectively $0.51 \cdot 10^8$, $0.67 \cdot 10^8$, and $0.62 \cdot 10^8$ for a total moment of $1.8 \cdot 10^8$ gauss cm³.

(S) Minuteman calculations were made on the basis of similar assumptions and the same tables for a total site weight of 257 tons with 30 tons in the launch tube at an L/D of 5 and the balance of 227 tons distributed for an L/D of unity giving $9.3 \cdot 10^6$ and $11.6 \cdot 10^6$ respectively for a total moment of $2.1 \cdot 10^7$ gauss cm³.

(S) The theoretical moment of 395-C as listed in Table 3 is lower than the measured value by nearly an order of magnitude, and the theoretical moment for a typical MM silo at Whiteman is about one third of the measured values. The figures used for material distribution for calculating the L/D ratio are approximations and could be responsible for some of the observed differences as could the assignment of numerical values for induced magnetic moments as a function of volume and shape. Differences of nearly an order of magnitude have been observed in the induced moment per unit ton of ferromagnetic material having roughly the same external shape and volume but containing different internal material distributions or having different magnetic histories.

(S) Measured values of MM 05 and MM 22 obtained at Vandenberg AFB are at least an order of magnitude larger than the measured MM values at Whiteman AFB. Figure 2 shows that the signals from MM 05 and MM 22 are likely to be disturbed by the signals from other close by silos, by the susceptibility contrasts of the water-beach interface and by the abruptly rising hills east and north of the sites. It is also likely that signal amplitudes for these two units may have been enhanced as a result of repeated missile launches from these units with their attendant high temperatures, pressures, and shock and vibration levels.

(S) The magnetic moment of the Russian built ZIL-157 truck computed using position 2 of Gauss, was in general agreement with the values obtained earlier for

SECRET

12

plot but there was a tendency for the observed signal period to be longer than its predicted value, probably as a result of the combined effects of the filters, pen-amplifiers and pen-paper friction. It should be noted that if the low frequency cutoff of the filter is approximately equal to the target profile period, the observed period will be less than the true period; and if the high frequency cutoff is about equal to the target profile period, the observed period will be longer than the true period.

3.1.1 MOMENT DETERMINATIONS AND PREDICTIONS

(S) Moment calculations for the target silos were made in simplified form using the expression for the first position of Gauss: $H = 2M/d^3$, where H represents peak-to-peak signal amplitude observed by the magnetometer as it passed over the target at a distance d from target center to sensor. M is the magnetic moment of the target. Use of the above equation depends on the assumption that M is aligned with the silo's long axis, that this axis is vertical, and that the sensor is seeing the total signal, not just the vector sum of the earth's field and the perturbing signal of the silo. These assumptions are not wholly valid but, at the range of dip angles experienced, are not likely to be in error by more than a factor of 2. Table 3 lists the results obtained by this method.

Table 3. Magnetic Moments of Various Targets (S)

Area	Target	Moment (gauss cm ³)	Method
Vandenberg AFB	Titan 395-C	$1.2 \pm .3 \cdot 10^9$	Airborne Measurement (apx)
Vandenberg AFB	Titan 395-C	$1.8 \cdot 10^8$	Theoretical Approximation
Vandenberg AFB	Titan 395-C	$0.8 \pm .1 \cdot 10^9$	Airborne Measurement (apx)
McConnell AFB	Titan 3-6	$1.0 \pm .2 \cdot 10^9$	Airborne Measurement (apx)
McConnell AFB	Titan 3-5	$1.3 \pm .3 \cdot 10^{9+}$	Airborne Measurement (apx)
Vandenberg AFB	MM 05	$4 \cdot 10^3$	Airborne Measurement (apx)
Vandenberg AFB	MM 22	$0.7 \cdot 10^9$	Airborne Measurement (apx)
Whiteman AFB	MM F8	$0.7 \pm .4 \cdot 10^8$	Airborne Measurement (apx)
Whiteman AFB	MM F9	$1.4 \pm .6 \cdot 10^8$	Airborne Measurement (apx)
Whiteman AFB	MM -	$2.1 \cdot 10^7$	Theoretical Approximation
Kirtland AFB (Stallion)	ZIL-157	$0.9 \pm .6 \cdot 10^6$	Airborne Measurement (apx)

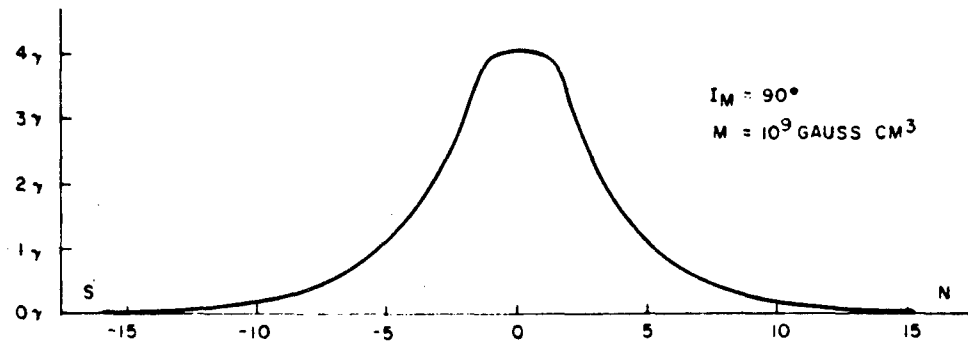
* The silo blast door (containing 700 tons of steel) was in the open position.

SECRET

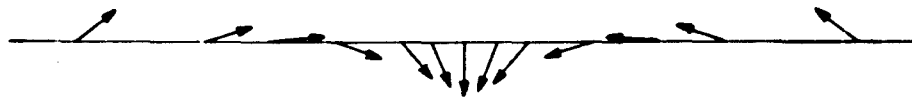
SECRET

(This page is unclassified)

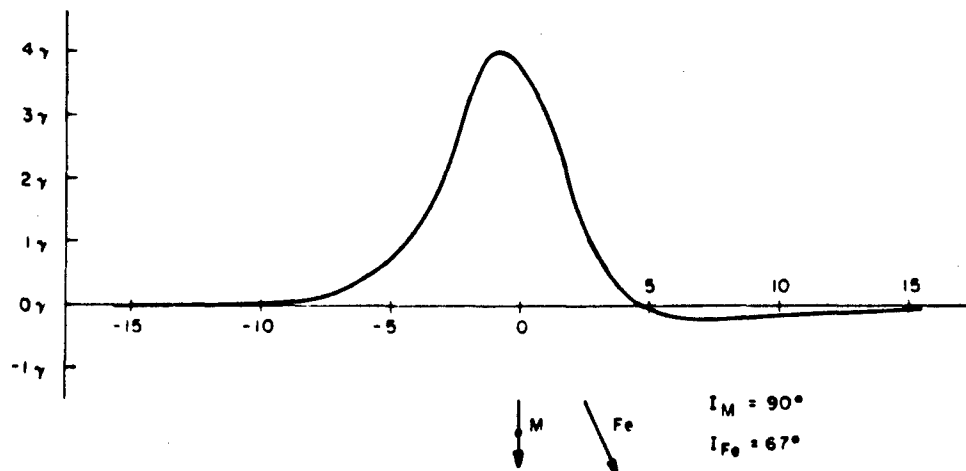
15



(a) Signal Amplitude



(b) Signal Direction



(c) Resultant ARMS Signal for $I_{Fe} = 67^\circ$

Figure 7. Signal Characteristics vs Time in Seconds (U)

SECRET

SECRET

14

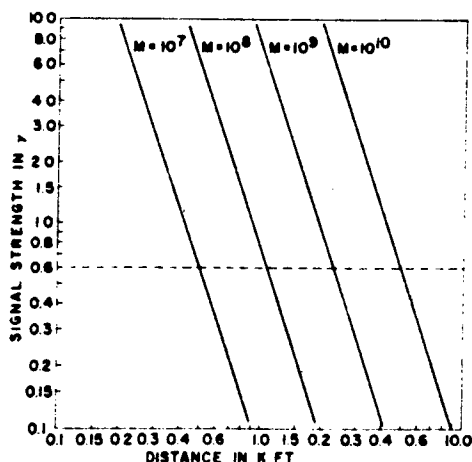


Figure 6. Signal Strength vs Target Distance (U)

similar U.S. vehicles being only slightly smaller. However, the spread in the observed data, particularly as a function of heading and the high background noise levels in the area, suggested a need for further testing. This was done at a later date and data and findings are presented as Appendix A to this report.

(S) Figure 6 is a plot of signal amplitude in gammas vs distance in thousands of feet for various dipole moments assuming the most favorable orientation. The dashed line represents a signal amplitude of 0.6γ , three times the typical observed background noise for straight and level flight in the vicinity of McConnell AFB measured

in a bandpass of 0.025 to 1.0 Hz at a distance above the ground of over 2000 ft and at a ground speed of 140 knots. The 3X noise-level line is significant as it indicates the required target signal amplitude for recognition by an operator with only minimal training. It was also observed that the noise level in the above bandpass did not increase at the 1500 ft level and decreased nearly 50 percent at the 3000 ft level.

(S) It is obvious that the actual induced dipole field for any launch site having a considerable lateral extent and located within the range of dip angles experienced in the United States will have a dip angle of its own and that this dip angle will be close to the angle of the inducing field. The ARMS magnetometer responds only to changes in the magnitude of the total magnetic field vector, and hence sees only the projection of the anomalous field vector onto the ambient earth's field vector. Figure 7(a) is a plot of the absolute amplitude in gammas vs time in seconds calculated for a south to north pass over a target of moment $M = 10^9$ gauss cm^3 . It was assumed that M dipped 90° below the horizon, that the aircraft was above the target at zero seconds, the aircraft ground speed was 140 knots, and altitude above the target was 1200 ft. Heading, ground speed, and altitude correspond to the values for pass No. N8 at McConnell AFB over Titan II silo 3-6. Figure 7(b) shows the direction of the anomalous signal vector as a function of time and hence distance along the flight path and Figure 7(c) shows the profile that the ARMS magnetometer would see flown over the same target with a background field dip angle equal to 67° .

SECRET

pass No. N8 through the Varian bandpass filter set for 0.015 to 1.0 Hz and corrected for base line variation. The shape and amplitude of the first half of the computed and measured curves are in close agreement. The second half of the measured curve, though similar in shape to the computed curve, shows a much larger negative going swing than its computed counterpart, most likely as a result of driving the bandpass filter to near saturation, thus creating a tendency for it to ring at its characteristic frequency.

3.1.2 FILTER SELECTION AND OPTIMIZATION

(C) Successful utilization of the ARMS system in a real-time mode and operated by aircrewman requires a displayed signal having the maximum possible signal to noise ratio. Automatic feature recognition systems and/or after-the-fact data processing procedures work best when the entire signal energy is recovered as completely as possible. In order to optimize signal to noise ratios the data from each individual pass was processed as indicated in Section 3.1. Figure 9 shows relative noise and signal + noise levels vs individual half-octave bandpass filters as listed in Table 1. Curve set (a) gives average values for a total of eight passes over site 395-C, two passes each on the four cardinal headings. Set (b) represents a similar series of passes over 395-D. The sharp signal peak in (b) using filter No. 3 is immediately evident. It can be seen that noise levels are at a minimum in the passband of filter No. 7 and that the noise increases steadily with lower frequency passbands. A small increase with higher frequencies is also evident. These increases can be attributed respectively to a combination of local geology and aircraft maneuver noise and to aircraft mechanical and electrical systems noise. Sites C and D are nearly adjacent and are located such that both geologic and man-made noise levels are similar, hence the only remaining parameter that could be responsible for the observed signal differences is the initial ARMS filter setting for the tape recording from which the half-octave information was obtained.

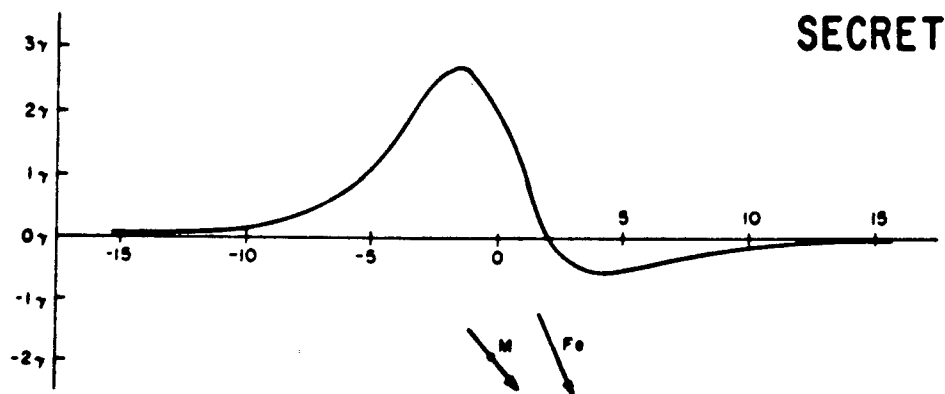
(S) Set (a) was recorded through a bandpass of 0.015 to 1.0 Hz and (b) through 0.035 to 1.0 Hz. That the reduced bandwidth improves the observed signal + noise to noise ratio by lowering the overall noise level is evident from comparison of the noise curves of (a) and (b). The effect of reduced initial low frequency bandwidth was checked by plotting another set of data obtained over site 395-C. Using two sets of cardinal heading passes, a distance of 2200 feet from the on-top sensor to the target dipole center, a ground speed of 135 knots, and a bandpass of 0.025 to 1.0 Hz, an analysis of the half-octave filter set output showed results comparable with those of Figure 9(b). Minimum noise occurred in the passband of filter No. 7 and a strong signal amplitude peak within the passband of filter No. 3. The overall shape of both the noise and the signal + noise curves was very similar to that of 9(b).

SECRET

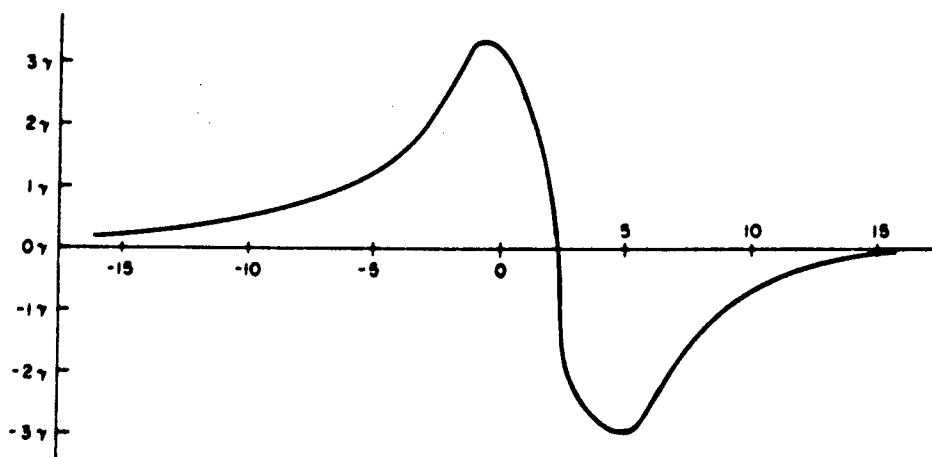
16

(C) Note that the amplitude of the profile as seen by the ARMS is nearly the total signal of the source dipole but that the profile appears sharper (higher frequency), its peak occurs prior to the on-top point, and that the tail-off goes negative.

(S) Figure 8(a) is a plot based on the general conditions of pass No. N8 with the additional assumptions that the dipole is located 65 feet below the surface, that the value of M is 10^9 gauss cm^3 and is dipping to the north at an angle of 50° in an ambient field dipping 67° . Figure 8(b) is a plot of the actual data obtained for



(a) Computed for $I_m = 50^\circ$ and $I_{Fe} = 67^\circ$



(b) Measured for Pass Number N8

Figure 8. ARMS Signal vs Time (U)

SECRET

SECRET

19

(S) Figure 10 is a plot of half octave filter numbers vs altitude for two curves: the filter number for maximum observed signal + noise to noise ratio and the filter number in which the maximum signal, including noise was observed. Each plotted point represents an average of several passes (normally four or eight) over the target at the same altitude. Average ground speed for the plots was 130 knots and ranged from 115 to 145 knots. Referring to Table 1 and the curves of Figure 5, it can be seen that the purely theoretical value for a given set of conditions generally lies between the two curves plotted in Figure 10. Therefore the optimum filter selection for a given set of search conditions for visual recognition by an aircrewman would be one filter number higher than the filter arrived at from use of the curves of Figure 3 and Table 1. An automatic or post-flight recognition could best be obtained by recording or processing the signal through a passband equivalent to three adjacent half-octave filters, the center filter frequency band containing the value arrived at from the curve sets of Figure 3.

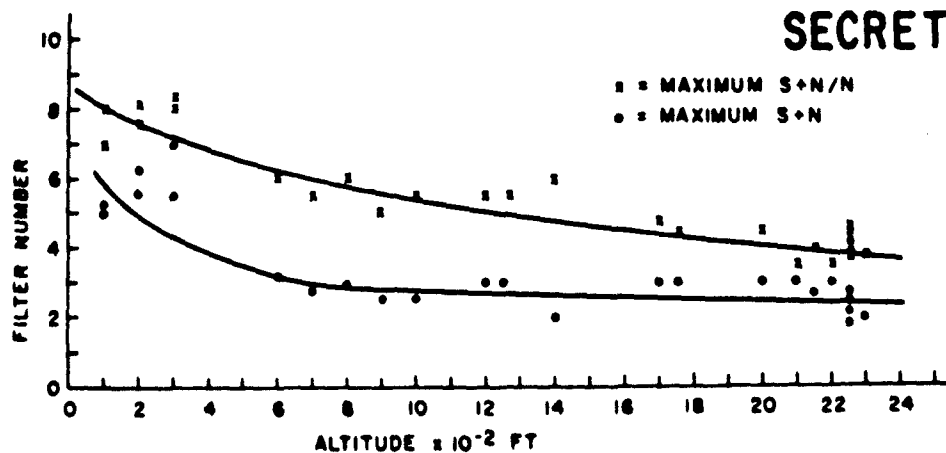


Figure 10. Filter Number vs Altitude for Maximum Signal and Signal/Noise(U)

SECRET

SECRET

18

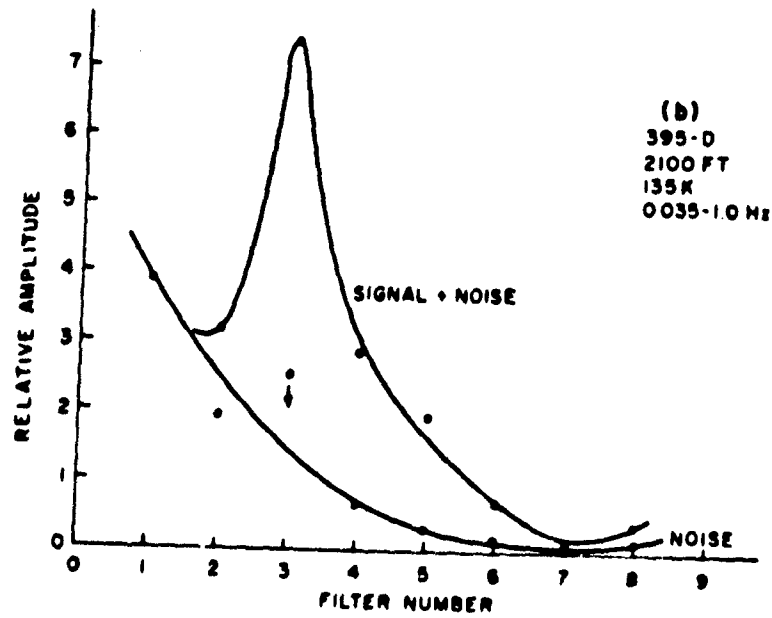
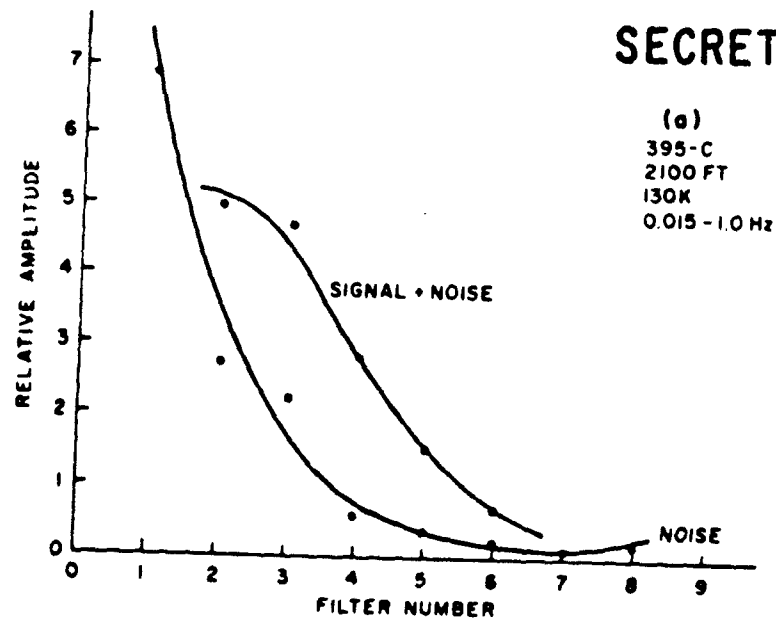


Figure 9. Relative Signal + Noise and Noise Levels vs Filter Numbers (U)

SECRET

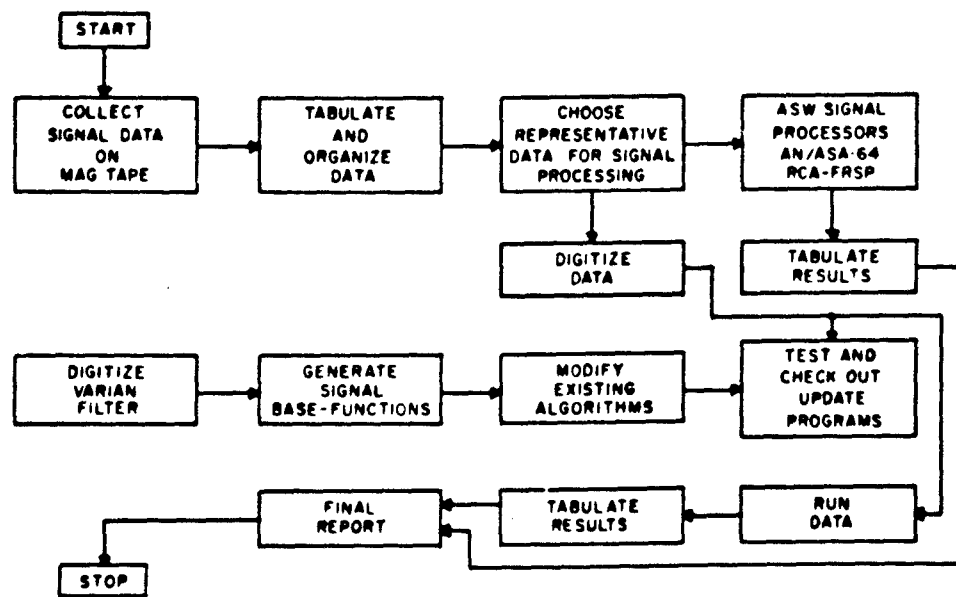


Figure 11. NADC Data Analysis Flow Chart (U)

Table 5. NADC Target Dipole Moments (U)

Target	Dipole Moment (Gauss - cm ³) ¹	Moment Elevation Angle	Location
395C	$1.447 \pm .120 \times 10^9$	-52.9°	Vandenberg AFB
395D	$1.041 \pm .149 \times 10^9$	-44.8°	
MM 05	$1.466 \pm .342 \times 10^{10}$	-50.0°	
3-6	$1.430 \pm .319 \times 10^9$	-51.8°	McConnell AFB
F-9	$1.683 \pm .597 \times 10^8$	-41.1°	Whiteman AFB

* Moment (±) error interval is based on t-test for 95 percent confidence interval.

3.2 NADC Procedures

(S) The principal data reduction goals for the Project EGAD work effort at NADC Johnsville were:

- (a) To determine the magnetic character of the targets, and
- (b) To study the applicability of previously developed ASW signal processing techniques to the EGAD data.

In Table 4 the data examined is summarized and Figure 11 is a flow chart of the general analysis procedure. Data obtained from passes over the ZIL truck were not tabulated or analyzed at NADC and some passes flown were not included in the data summary due to various conflicts such as target background ambiguities or to instrumental difficulties. Table 5 lists target dipole moments as presented in the NADC final report by Schneider (1970). The magnetic moment figure for target MM 05 is reported to be less reliable than the others included because the signal passes were on a single heading. Target F-8 was not included because the data was inconsistent as evidenced by a high standard deviation.

Table 4. NADC Data Collection Summary

Target	No. of Signals	Location
395C	29	Vandenberg AFB
395-D	27	
MM 05	24	
3-6	40	McConnell AFB
3-5	7	
3-4	2	
3-7	1	
3-9	1	
F-8	24	Whiteman AFB
F-9	18	
F-7	1	
F-5	1	
I-3	1	
I-2	1	
	<hr/> 178	

SECRET

22

(C) Three ASW signal processing techniques for semi-automatic and fully automatic signal recognition were applied to portions of the EGAD data. In Table 6 the outputs of these methods are listed. The results although essentially qualitative, demonstrate the feasibility of using previously developed signal recognition techniques appropriately optimized for application to EGAD type data. Technical discussions of the methods used for analysis of the EGAD data and the signal processing techniques applied are contained in Schneider (1970).

Table 6. Auto-Detection of EGAD Targets

Processor Type	No. Signals	No. Hits	No. False Alarms	Recognition Rate	False Alarm Rate
AN/ASA-64 Submarine Anomaly Detector	12	11	21	0.917	1.75
RCA-FRSP (Feature Recognition Processor)	32	20	8	0.625	0.25
AFFP-Anderson Function Fitting Processor	9	9	2	1.00	0.22

I. CONCLUSIONS

(S) The dipole magnetic moments of various Titan II and Minuteman launch silos and the direction of these moments as found by AFCRL and by NADC using the same data but proceeding independently generally show good agreement. The magnetic moments of these sites as determined from such considerations as volume and distribution of ferromagnetic materials and various assumed magnetization factors is nearly an order of magnitude too low. This can be improved by using a larger length to diameter ratio obtainable as a result of converting the mass of the launch tube cylinder to an equivalent mass having a solid cylindrical shape of nearly equivalent length. It can be concluded that:

A. (S) Maximum detection range based on the dipole moment values of Tables 3 and 5 and on an assumed systems sensitivity of 0.1 gamma peak-to-peak representing signal processing techniques optimized for EGAD type targets in areas of low and moderate geologic noise is:

- (1) 4000 ft for Titan II sites,
- (2) 2100 ft for Minuteman sites.

SECRET

B. (S) Maximum detection range based on an assumed systems sensitivity of 0.3 gamma representing the capability of human operators and visually displayed signals is:

- (1) 2900 ft for Titan II,
- (2) 1400 ft for Minuteman.

C. (S) There is no observable difference between loaded or unloaded and fired or unfired silos.

D. (S) Aeromagnetic survey aircraft operating in areas of moderate to high geologic noise can realize an increase in human operator detection range by using as high a ground speed as possible consistent with low aircraft magnetic noise levels.

E. (C) Extension of current capabilities to areas of high geologic noise without loss of range would require development of improved noise rejection methods.

5. APPLICATIONS

(S) Missile site detection and the use of a site's magnetic signature as a terminal guidance device are limited by the maximum ranges previously cited (less than one mile) but there are conditions under which this limited range could be useful. These include detection within supposed neutral or "friendly" areas subject to weapons ban treaties without violating a nation's ground sovereignty and as a post strike reconnaissance tool over an aggressor's territory.

(S) The major use of systems such as ARMS and EGAD lies in their ability to detect ferromagnetic objects such as trucks, truck parks, pipe lines, and weapons storage caches, particularly when buried or concealed by darkness or jungle cover. Project Iron Barnacle, NADC (1970), a program of airborne magnetic detection in Vietnam and Cambodia, was responsible for the location and eventual destruction and/or capture of five major ordnance caches, a training base, an artillery base, and several vehicle repair stations.

(C) The joint NADC-AFCRI land target programs contributed to the success of this operation by providing background information on signal characteristics and geologic noise levels, by providing for land target filter parameter studies and by encouraging land target detection via magnetics. Problem areas encountered included navigation and target marking and the recorder-display system. It should be noted that the ARMS split-memory dual-beam cathode-ray system is ideal for this type of operation permitting simultaneous display of the signals from each of several previous passes plus a detailed display of the pass in progress.

SECRET

(This page is Confidential)

24

6. RECOMMENDATIONS

(C) It has been demonstrated that airborne magnetic detection can be used with considerable success for the detection of hidden, buried, or otherwise concealed targets of military significance. There are several ways in which existing systems can be improved leading to increased range or to increased reliability of target identification. These include but are not limited to the following:

A. (U) Development and flight testing of a new single cell orienting magnetometer system now being investigated jointly by the Canadian Armed Forces and CAE Electronics, Ltd. This unit shows promise of reducing instrument electronics noise and maneuver noise to levels lower than those of the ARMS or AN/ASQ-81 multiple cell sensors. It also operates over wide temperature ranges and with a faster warm up time than the existing ARMS units.

B. (U) Development of signal digitization and real time small scale computer procedures to permit optimization of signal processing techniques for land target applications.

C. (C) Adaptation of existing navigation systems to a configuration that would permit flying an aeromagnetic survey aircraft over the same path with very close tolerances, thus permitting differences in magnetic signals to be obtained for successive passes and to be processed automatically identifying any change in the magnetic background even in the presence of a naturally noisy environment.

D. (U) Design, development, and/or modification of existing Air Force aircraft incorporating the features of A, B, and C above plus devices such as the AN/A5A-63 automatic magnetic compensator and the CAE magnetic anomaly simulator. Acquisition of an existing or in-procurement Navy aircraft designed specifically for ASW warfare and modification of such aircraft for land target acquisition. The Air Force North American OV10A and the Navy S3A are recommended, respectively.

SECRET

Acknowledgments

The assistance of the scientific and flight personnel of the Naval Air Development Center, Johnsville, Pennsylvania, and of the Navy and Air Force bases from which operations were conducted, is gratefully acknowledged. Special thanks are given to Lt. Col. Leon Stone, AFCRL, for the initial suggestions on which this program was based, and for his encouragement and interest throughout its execution.

References

- Maple, E. (1966) Aerial Magnetic Detection in Counter-Insurgency Warfare - A Preliminary Technical Report, Air Force Surveys in Geophysics, No. 172. Unclassified.
- McBride, R. A. (1967) Airborne Reconnaissance Magnetometer System, Final Report, AFCRL 67-0694, Contract AF19(628)-67-C-0144. Confidential.
- McBride, R. A. (1968) Airborne Reconnaissance Magnetometer System, Supplement to the Final Report, AFCRL 68-0359, Contract AF19(628)-67-C-0144. Confidential.
- NADC (1970) Land Target MAD In Southeast Asia, NAVAIRDEVCON AEYM (18/8/70). Secret.
- Schneider, R. J. (1970) Final Report on Project EGAD, NAVAIRDEVCON AEYM (11/25/70). Secret.
- Zawalick, E. J., and Hutchinson, R. O. (1970) Aerial Magnetic Detection in Counter-Insurgency Warfare Part II, Experimental Results, Air Force Surveys in Geophysics, No. 215, AFCRL-70-0096. Secret.

SECRET

29

Appendix A**ZIL Signatures**

(S) The Foreign Technology Division, Air Force Weapons Laboratory, KAFB, New Mexico, obtained a Russian ZIL-157, 6 by 6 truck and has conducted a program known as Project Have Vase to define the properties of the vehicle relating to its detection in SEA and elsewhere. Because it is known that over 2400 of these trucks are operating on the supply routes from North Vietnam through Laos and Cambodia into the RVN their overall signatures are most important. Parameters measured included IR reflectivity, radar cross-section measurements, paint composition, metallurgical factors, magnetic moments, and seismic signatures. AFCRL, through Project EGAD obtained a series of airborne magnetic signatures from the truck in July 1969. The flights made within the White Sands Missile Range indicated that the overall magnetic moment of the truck was smaller than would be expected from a vehicle of its size and weight. It was postulated that the vehicle was degaussed prior to delivery or that it was assembled using practices and materials unfamiliar to us. Additional studies of the data obtained showed a high area noise level which may also have masked a portion of the truck's signature.

(S) It was decided to obtain more accurate measurements of the total moment of the vehicle, to provide estimates of the relative strength of the induced and permanent portions of the field and to make these determinations in such a manner that they would not be adversely affected by local geologic noise. A remote, smooth surfaced, hard packed area in the gypsum sands section of the WSMR was selected for operations. Geologic noise was minimized by reason of the uniform nature of

SECRET

the soil material and man made disturbances by blocking access roads to the area and by operating on a small portable power unit. A magnetic N-S line was established and a three component fluxgate magnetometer set at a height corresponding to the center of gravity (CG) of the vehicle was centered over the line. Overall systems sensitivity including effects of temperature, wind loading (tilt) and electronics noise was less than $\pm 1.0\%$. Effects of diurnal field changes were minimized by keeping measurement intervals as short as possible. It was also determined that the magnetic center for the vertical component corresponded to the truck's CG and that a dipole field approximation was valid for a separation distance of 60 ft between the truck's CG and the sensor elements.

(S) The truck (CG) was placed over a stake 60 feet south of the sensor and was carefully aligned on a north heading. The magnetic elements x, y, z were read and recorded and the truck was rapidly driven about 500 yards away from the sensor. The unbiased x, y, z elements were read and recorded. The procedure was repeated for truck headings of east, south, and west and for a similar set over a stake 60 feet north of the sensor. The results are shown below.

(S) Experimental measurements in gamma (γ) for a ZIL-157 truck located 60 ft south of the magnetometer.

Vehicle Heading	<u>X</u>	<u>Y</u>	<u>Z</u>	<u>F</u>	<u>M (gauss cm³)</u>
N	9.5	-2.5	-12.5	15.9	$8.32 \cdot 10^5$
E	6.0	5.0	-13.5	15.6	$8.99 \cdot 10^5$
S	29.5	1.5	-12.5	32.1	$11.86 \cdot 10^5$
W	14.	-5.	-12.	19.1	$9.03 \cdot 10^5$
Average					$M = 9.55 \cdot 10^5$

(S) ZIL-157 truck located 60 ft north of the magnetometer.

Vehicle Heading	<u>X</u>	<u>Y</u>	<u>Z</u>	<u>F</u>	<u>M (gauss cm³)</u>
N	12.5	-2.5	-12.0	17.5	$8.42 \cdot 10^5$
E	9.5	3.5	-12.0	15.7	$8.18 \cdot 10^5$
S	26.5	1.0	-12.0	29.1	$10.95 \cdot 10^5$
W	14.5	-3.0	-11.0	18.4	$8.26 \cdot 10^5$
Average					$M = 8.95 \cdot 10^5$

(S) Each experimental value represents the difference in value between the unbiased field and the field with the truck present and is an average of three or more separate determinations. The total spread for each was about $\pm 1\%$. The F value is total field change in gammas and has been computed from

$F = \sqrt{x^2 + y^2 + z^2}$ and $M = r^3 \sqrt{x^2/4 + y^2 + z^2}$. A similar set of data obtained at L. G. Hanscom Field from a standard 2 1/2 ton Army vehicle taken 60 feet to the South of the magnetometer is given below.

(S) Two and a half ton Army truck located 60 feet south of the magnetometer.

Vehicle Heading	<u>X</u>	<u>Y</u>	<u>Z</u>	<u>F</u>	<u>M (gauss cm³)</u>
N	16.5	0	-18.3	24.6	$1.23 \cdot 10^6$
E	8.5	-2.0	-18.0	20.0	$1.14 \cdot 10^6$
S	10.1	0	-19.8	22.2	$1.25 \cdot 10^6$
W	9.4	2.1	-19.0	21.3	$1.20 \cdot 10^6$
Average					$M = 1.21 \cdot 10^6$

(S) It should be noted that for this set the values of the inducing fields, respectively for x and z, were 16,900 γ and 52,500 γ , where the equivalent WSMR values were 24,650 and 43,500 γ . The data presented was read to 0.1 γ but is significant only to 0.5 γ . Readings were obtained from five identical trucks and represent the set closest to the mean values of the group.

(S) A complete numerical solution for the parameters required to identify the permanent and induced components of an object's magnetic field normally required that the direction of the inducing field with respect to the vertical axis of the object be reversed during the data collection process. This could have been accomplished by turning the truck upside down or by making additional measurements in latitudes where the dip angle direction is reversed. These actions are difficult and not needed for we can infer several things from the shape of the vehicle and from the tables.

(S) The shape of the truck's frame members suggests that maximum induced magnetization will occur in the longer horizontal dimension when the truck is pointing N or S. The first data set shows this and shows that maximum moment occurs when the vehicle is heading south. We can assume that the induced x component x_i and the permanent x component x_p are additive: $x_i + x_p = \Delta x = 29.5\gamma$; and for a north heading $x_i - x_p = \Delta x = 9.5\gamma$; and by adding $2x_i = 39\gamma$, $x_i = 19.5\gamma$ and $x_p = 10\gamma$. Noting that the long dimension of the truck is its x axis and that the sensor x, y, z axes are fixed we see from the E and W heading data of set 1 that the truck's permanent field in its X direction as seen at 60 ft is 10 γ and is directed toward the rear of the truck. The induced field when the truck is aligned with the earth's field's horizontal direction is 19.5 γ , and when the truck is at right angles to this direction it is about 9 γ .

(S) The y component of the truck's permanent field is smaller appearing as 2 or 3 γ signal at 60 ft and is directed toward the right-hand side of the vehicle.

As mentioned earlier, it isn't possible to separate the z component permanent and induced fields from the given data. This could affect the estimates of the above values by small amounts but probably by not more than $\pm 2\gamma$.

Conclusions:

(S) The average total magnetic moment of the 11,600-lb ZIL truck was $9.55 \cdot 10^5$ cgs units measured at WSMR. The average value for a 12,400 lb two and a half ton U.S. vehicle was $1.21 \cdot 10^6$ cgs units measured at Hanscom Field and equivalent to $1.37 \cdot 10^6$ units measured at WSMR. The ZIL value was 70 percent of its U.S. equivalent although it weighed 94 percent of its counterpart. The ratio of permanent to induced fields for the ZIL was approximately 1 to 2; for its U.S. equivalent the ratio was 1 to 4.

(S) It can be concluded that:

- A. (S) The ZIL has not been degaussed.
- B. (S) Its structural material, shape and assembly methods have produced a large permanent magnetic field component along its major axis.
- C. (S) It is more difficult to induce magnetic field components along its axis than its U.S. counterparts.
- D. (S) Carefully placing the ZIL truck on a heading such that its induced and permanent horizontal moments are directed oppositely will reduce its net moment and hence the range at which it could be found with MAD type devices.

(S) These results and conclusions have been published as a portion of Air Force Systems Command Foreign Technology Document, "Exploitation of Project Have Vase", dated 24 April 1970.

Unclassified
Security Classification

DOCUMENT CONTROL DATA - R&D		
<i>(Security classification of title, body of abstract and indexing annotation must be entered when the overall report is classified)</i>		
1. ORIGINATING ACTIVITY (Corporate author) Air Force Cambridge Research Laboratory (PHG) L.G. Hanscom Field Bedford, Massachusetts 01730		2A. REPORT SECURITY CLASSIFICATION Secret
		2B. GROUP 1
3. REPORT TITLE PROJECT EGAD, EXPLORATORY GEOPHYSICAL ANOMALY DETECTION(U)		
4. DESCRIPTIVE NOTES (Type of report and inclusive dates) Scientific Interim		
5. AUTHOR(S) (First name, middle initial, last name) Robert O. Hutchinson		
6. REPORT DATE 30 March 1971	7A. TOTAL NO. OF PAGES 37	7B. NO. OF REFS 6
8A. CONTRACT OR GRANT NO. A. PROJECT, TASK, WORK UNIT NOS. ILIR0001 Task 9-69 C. DOW ELEMENT 61101F D. DOD SUBELEMENT 680100		9A. ORIGINATOR'S REPORT NUMBER(S) AFCRL-71-0221 9B. OTHER REPORT NUMBER(S) (Any other numbers that may be assigned this report) AFSG, No. 233
10. DISTRIBUTION STATEMENT 4-In addition to security requirements which apply to this document and must be met, each transmittal outside the Department of Defense must have prior approval of AFCRL, XO, L.G. Hanscom Field, Bedford, Massachusetts 01730		
11. SUPPLEMENTARY NOTES This research was supported by the Air Force In-House Laboratory Independent Research Fund.		12. SPONSORING MILITARY ACTIVITY Air Force Cambridge Research Laboratory (PHG) L.G. Hanscom Field Bedford, Massachusetts 01730
13. ABSTRACT (U) An airborne reconnaissance magnetometer system (ARMS) was installed in a Grumman Tracker (S2E) aircraft in a joint program with the Naval Air Development Center, Johnsville-Warminster, Pa. Signatures were obtained from targets of special interest and magnetic moments were computed from the flight data and compared with values derived from theoretical considerations. Signal amplitude, noise amplitude, signal period, and relative signal-to-noise ratio were obtained for each signature by passing the recorded signals through a series of half-octave filter steps. Suggestions for optimum filtering are presented. Anti-Submarine Warfare (ASW) signal processing techniques were investigated to determine their usefulness for land target identification. Applications of the ARMS and EGAD systems and recommendations for future investigations are given.		

DD FORM 1473
NOV 66

Unclassified
Security Classification



Unclassified
Security Classification

14. KEY WORDS	LINE A		LINE B		LINE C	
	ROLE	WT	ROLE	WT	ROLE	WT
MAD Magnetic Airborne Detection Magnetometer Magnetic Moment ASW Surveillance						

Unclassified
Security Classification

This page is unclassified

SUPPLEMENTARY

INFORMATION



DEPARTMENT OF THE AIR FORCE
PHILLIPS LABORATORY (AFMC)

ERRATA
AD-517038

E 9 JUL 1995

MEMORANDUM FOR DEFENSE TECHNICAL INFORMATION CENTER (DTIC)
8725 John J. Kingman Road
Suite 0944
Fort Belvoir, VA 22060-6218

FROM: OL-AA PL/GPS
29 Randolph Road
Hanscom AFB MA 01731-3010

SUBJECT: Document Declassification and Distribution Statement
Change

1. I have reviewed the following documents and have determined that the classification and distribution statement on these documents are no longer appropriate:

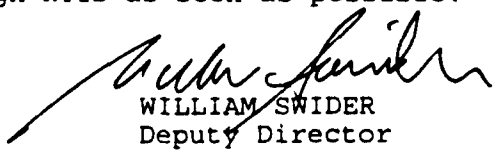
a. Number: AD508283
Title: Aerial Magnetic Detection in Counter-Insurgency Warfare, Part II, Experimental Results
Authors: Zawalick, Edward J. and Hutchinson, Robert O.
Report No: AFCRL-AFSIG-215, AFCRL-70-0096
Report Classification: CONFIDENTIAL

b. Number: AD517038
Title: Project EGAD, Exploratory Geophysical Anomaly Detection
Author: Hutchinson, Robert O.
Report No.: AFCRL-AFSIG-233, AFCRL-71-0221
Report Classification: SECRET

2. Request these reports be declassified and assigned Distribution A Statement.

3. This action is in response to a FOIA request. The requestor wishes to purchase a copy of the technical reports through NTIS. Please expedite processing the declassification of these reports so they may become available through NTIS as soon as possible.

ERRATA


WILLIAM SWIDER
Deputy Director
Space Physics Division

CC:
PL/TL